Physicalized Temperature: A New Correlation Mechanism Between ^{4}He Atoms

Di Zhuang* and Hongzhang Zhuang†
Metal Laboratory, American Axle and Manufacturing Inc., 455 Gibraltar Drive, Bolingbrook, 60440 Illinois USA

The experiment shows that in the superfluid ^{4}He, ^{4}He atoms are not an ideal Bose gas, and there is a strong correlation between the ^{4}He atoms in the superfluid state. The famous Tisza and Landau's two-fluid model does not provide an answer to the physical mechanism behind this correlation. This paper proposes a hypothesis—Physicalized Temperature (PT), a specific mechanism for the correlation between ^{4}He atoms. Based on this model, new explanations are given for critical opalescence and the quantization of circulation; it is also predicted that, similar to superconductors, magnetic flux quantization will occur in a rotating torus container filled with superfluid ^{4}He. The phonon-roton dispersion curve (P-R curve) of the superfluid ^{4}He quasiparticles, which was conjectured by Landau, as well as the specific heat curve with singularities across the entire temperature range, are calculated and found to match the experimental data very well.

I. INTRODUCTION

Since the discovery of superfluidity in helium, a large number of theoretical studies have emerged to explore its microscopic mechanisms. Among them is the famous Tisza[1] and Landau's[2] two-fluid model. Although this theory can explain some experimental phenomena, it also presents many unresolved mysteries. For example, at the λ point, numerous experiments have confirmed the singularity of the specific heat, yet according to Landau's theory, the specific heat should be finite. Although he speculated about the phonon-roton dispersion curve (P-R curve)[3] in superfluid ^{4}He quasiparticles, unfortunately, it has still not been possible to calculate this curve based on Landau's theory. Furthermore, the physical picture of the so-called rotons is also unclear. Experiments have repeatedly shown that in the superfluid ^{4}He, ^{4}He atoms are no longer an ideal Bose gas, and there is a strong correlation between the ^{4}He atoms in the superfluid state. The most regrettable aspect is that Landau's two-fluid model does not answer why, when the temperature drops to T_λ, a sudden strong long-range correlation appears between the ^{4}He atoms, let alone provide a physical mechanism for this correlation.

Additionally, a phenomenon that is strikingly similar to the behavior of ^{4}He at the λ point is the critical phenomenon. The currently considered most successful theory for this phenomenon is the renormalization group (RG)[4, 5] framework. It includes three pillars: scaling, universality, and renormalization. However, this theory cannot explain, from a physical mechanism perspective, why long-range correlations suddenly appear in the system when the temperature drops to T_c[6]. At the λ point and critical point, the behavior of ^{4}He atoms shares both similarities and distinct characteristics. For example, both show long-range order and specific heat divergence, but one is superfluid and the other is not; one exhibits opalescence, while the other does not. As a result, people believe that the physical mechanisms at the λ point and the critical point are different and require two distinct theories to describe them. However, in this paper, we propose a single hypothesis—Physicalized Temperature (PT)—as a specific mechanism for the correlation between ^{4}He atoms. It successfully describes the physical phenomena occurring at both of these phase transition points.

The structure of this paper is as follows. First, we assume that the annihilation of a photon in an $\hbar\mathbf{k}_\lambda$ and energy $\hbar\omega_\lambda$ mode leads to the creation of a derivative phonon (DP) with the same momentum and energy; Second, this DP couples with photons of other wavelengths at this temperature, and we derive the corresponding Hamiltonian. Fortunately, we have found the exact solution to this Hamiltonian, thus avoiding the need for the Green's function technique. A new concept, the physicalized photon (PP), is introduced. Third, we discuss various features of the exact solution and introduce the concept of physicalized temperature (PT); Fourth, based on this model, new explanations are given for critical opalescence and the quantization of circulation; it is also predicted that, similar to superconductors, magnetic flux quantization will occur in a rotating torus container filled with superfluid ^{4}He. The phonon-roton dispersion curve of the superfluid ^{4}He quasiparticles, as well as the specific heat curve with singularities across the entire temperature range, are calculated; Finally, we conclude the paper.

II. A HYPOTHESIS ON DERIVATIVE PHONONS AND THE EXACT SOLUTION OF THE HAMILTONIAN

Let us start from the cradle of quantum theory — blackbody radiation (BBR) with a cavity. To study the photon gas in the cavity, the vector potential $\boldsymbol{A}$ and its canonically conjugate momentum $\boldsymbol{P} = m_p\,\dot{\boldsymbol{A}}$, (where $m_p \equiv 1/4\pi c^2$ is the formal mass of photons, c is the speed

* kyxzbgzhz@gmail.com
† Correspondence should be addressed to the author zhzucf@gmail.com

of light in vacuum) are chosen as the variables. The photon Hamiltonian H_p, expressed in terms of the creation operator ($a^\dagger_{\mathbf{k}\sigma}$) and the destruction operator ($a_{\mathbf{k}\sigma}$) of the $\boldsymbol{A}(\boldsymbol{r})$ and $\boldsymbol{P}(\boldsymbol{r})$, is given by [7, 8]:

$$\begin{aligned} H_p &= \sum_{\mathbf{k}\sigma}[\frac{1}{2m_p}\Pi_A(\mathbf{k},\sigma)\Pi_A(-\mathbf{k},\sigma) \\ &\quad + \frac{1}{2}m_p\omega_k^2 A(\mathbf{k},\sigma)A(-\mathbf{k},\sigma)] \\ &= \sum_{\mathbf{k}\sigma}\hbar\omega_k(a^\dagger_{\mathbf{k}\sigma}a_{\mathbf{k}\sigma}+\frac{1}{2}) \end{aligned} \tag{1}$$

where

$$\begin{aligned} A(\mathbf{k},\sigma) &= \left(\frac{\hbar}{2m_p\omega_k}\right)^{1/2}(a_{\mathbf{k}\sigma}+a^\dagger_{-\mathbf{k}\sigma}) \\ \Pi_A(\mathbf{k},\sigma) &= -i\left(\frac{\hbar m_p\omega_k}{2}\right)^{1/2}(a_{\mathbf{k}\sigma}-a^\dagger_{-\mathbf{k}\sigma}) \\ \boldsymbol{A}(\boldsymbol{r}) &= \frac{1}{\sqrt{V}}\sum_{\mathbf{k}\sigma}\boldsymbol{e}_{\mathbf{k}\sigma}A(\mathbf{k},\sigma)e^{i\mathbf{k}\cdot\boldsymbol{r}} \\ \boldsymbol{P}(\boldsymbol{r}) &= \frac{1}{\sqrt{V}}\sum_{\mathbf{k}\sigma}\boldsymbol{e}_{\mathbf{k}\sigma}\Pi_A(\mathbf{k},\sigma)e^{i\mathbf{k}\cdot\boldsymbol{r}} \end{aligned}$$

Where $\omega_k = c\,|\mathbf{k}| = c\,k$, the V is the volume of the cavity. The $\boldsymbol{e}_{\mathbf{k}\sigma}$ is the unit vector and $\boldsymbol{e}^*_{-\mathbf{k}\sigma} = \boldsymbol{e}_{\mathbf{k}\sigma}$. The $\sigma = (1,2)$ denotes possible polarization directions of the photons. The commutation relations of the operators are $[A(\mathbf{k},\sigma),\Pi_A(-\mathbf{k}',\sigma')] = i\hbar\delta_{\mathbf{k}\mathbf{k}'}\delta_{\sigma\sigma'}$, $[a_{\mathbf{k}\sigma},a^\dagger_{\mathbf{k}'\sigma'}] = \delta_{\mathbf{k}\mathbf{k}'}\delta_{\sigma\sigma'}$.

Suppose we inject N_0 helium atoms into the cavity. We know that interactions occur both between the ^{4}He atoms within the cavity and between these atoms and the blackbody radiation, leading to changes in the thermal wavelength of ^{4}He and the speed of photons. At a density of ρ_λ and a temperature of T_λ, what physical processes within the system drive the superfluid transition of ^{4}He? We hypothesize that, at the lambda point, in the Planck distribution of bare photons at temperature T_λ, a photon with momentum $\hbar\mathbf{k}_\lambda$ and energy $\hbar\omega_\lambda$ suddenly annihilates upon interacting with ^{4}He, resulting in the creation of a phonon with the same momentum and energy. Since this special phonon is derived from the photon, we refer to it as a derivative phonon (DP), which is composed of N_λ of the N_0 helium atoms. The corresponding Hamiltonian, H_{dp}, is given by:

$$H_{dp} = \sum_j^{N_\lambda}\left(\frac{\boldsymbol{P}_j^2}{2m}+\frac{1}{2}m\,\omega_\lambda^2\boldsymbol{B}_j^2\right) \tag{2}$$

Where m is the mass of ^{4}He, $\boldsymbol{P}_j$ and $\boldsymbol{B}_j$ are momentum and amplitude of j-th ^{4}He in DP, respectively. Although it is a DP, unlike H_p, which only includes transverse waves, H_{dp} includes both transverse and longitudinal waves. Compared with regular phonons, DP has two special features. First, it is clear that DP represents a long-range order, a perfect crystal. However, since DP is uniformly intermingled with non-DP ^{4}He atoms, the system as a whole still appears disordered. The nearest neighbor ^{4}He atom of a ^{4}He atom in DP does not necessarily belong to DP, and the interaction between these two types of ^{4}He atoms causes the motion of ^{4}He atoms in DP to change from a harmonic oscillator to a damped harmonic oscillator. If this damping force is not very large, we can temporarily ignore it and discuss it later. Second, due to the appearance of a hole ($\hbar\omega_\lambda$) in the spectrum of T_λ, photons of other frequencies in the spectrum of T_λ will interact with DP, and we set the coupling constant between them as η. Since photons only couple to the transverse mode of DP, by hiding the longitudinal mode in Equation (2), H_{dp} becomes H_1:

$$H_1 = \sum_j^{N_\lambda}\left[\frac{1}{2m}\left(\boldsymbol{P}_j-\eta\boldsymbol{A}_j\right)^2+\frac{1}{2}m\,\omega_\lambda^2\boldsymbol{B}_j^2\right] \tag{3}$$

Using the following normal modes of the fields and their conjugate momenta,

$$\begin{aligned} B(\mathbf{k},\sigma) &= \left(\frac{\hbar}{2\,m\,\omega_\lambda}\right)^{1/2}(b_{\mathbf{k}\sigma}+b^\dagger_{-\mathbf{k}\sigma}) \\ \Pi_B(\mathbf{k},\sigma) &= -i\left(\frac{\hbar\,m\,\omega_\lambda}{2}\right)^{1/2}(b_{\mathbf{k}\sigma}-b^\dagger_{-\mathbf{k}\sigma}) \\ \boldsymbol{B}_j &= \frac{1}{\sqrt{N_\lambda}}\sum_{\mathbf{k}\sigma}\boldsymbol{e}_{\mathbf{k}\sigma}B(\mathbf{k},\sigma)e^{i\mathbf{k}\cdot\boldsymbol{R}_j} \\ \boldsymbol{P}_j &= \frac{1}{\sqrt{N_\lambda}}\sum_{\mathbf{k}\sigma}\boldsymbol{e}_{\mathbf{k}\sigma}\Pi_B(\mathbf{k},\sigma)e^{i\mathbf{k}\cdot\boldsymbol{R}_j} \end{aligned}$$

Where $\boldsymbol{R}_j$ is the Cartesian coordinate of j-th lattice point, the commutation relations of the operators are $[B(\mathbf{k},\sigma),\Pi_B(-\mathbf{k}',\sigma')] = i\hbar\delta_{\mathbf{k}\mathbf{k}'}\delta_{\sigma\sigma'}$, $[b_{\mathbf{k}\sigma},b^\dagger_{\mathbf{k}'\sigma'}] = \delta_{\mathbf{k}\mathbf{k}'}\delta_{\sigma\sigma'},(\sigma=1,2)$. The final Hamiltonian of the system combining Equation (1) and (3), $H = H_p + H_1$, is therefore

$$\begin{aligned} H = \sum_{\mathbf{k}\sigma}[&\hbar\omega_k(a^\dagger_{\mathbf{k}\sigma}a_{\mathbf{k}\sigma}+\frac{1}{2})+\hbar\omega_\lambda(b^\dagger_{\mathbf{k}\sigma}b_{\mathbf{k}\sigma}+\frac{1}{2}) \\ &+\frac{i}{2}\hbar\omega_p\left(\frac{\omega_\lambda}{\omega_k}\right)^{1/2}(b_{\mathbf{k}\sigma}-b^\dagger_{-\mathbf{k}\sigma})(a_{-\mathbf{k}\sigma}+a^\dagger_{\mathbf{k}\sigma}) \\ &+\frac{1}{4}\hbar\omega_p\frac{\omega_p}{\omega_k}(a_{\mathbf{k}\sigma}+a^\dagger_{-\mathbf{k}\sigma})(a_{-\mathbf{k}\sigma}+a^\dagger_{\mathbf{k}\sigma})\,] \end{aligned} \tag{4}$$

The quantity $\omega_p \equiv c\,\eta\sqrt{4\pi N_\lambda/mV}$. We will directly diagonalize H in four steps to obtain the eigenvectors and eigenvalues.

Step 1: We transform H into H_2 using the following scale transformations:

$$\begin{aligned} (a_{\mathbf{k}\sigma}+a^\dagger_{-\mathbf{k}\sigma}) &= \omega_k^{1/2}(\Xi_{\mathbf{k}\sigma}+\Xi^\dagger_{-\mathbf{k}\sigma}) \\ (a_{\mathbf{k}\sigma}-a^\dagger_{-\mathbf{k}\sigma}) &= \omega_k^{-1/2}(\Xi_{\mathbf{k}\sigma}-\Xi^\dagger_{-\mathbf{k}\sigma}) \\ (b_{\mathbf{k}\sigma}+b^\dagger_{-\mathbf{k}\sigma}) &= \omega_\lambda^{1/2}(\Theta_{\mathbf{k}\sigma}+\Theta^\dagger_{-\mathbf{k}\sigma}) \\ (b_{\mathbf{k}\sigma}-b^\dagger_{-\mathbf{k}\sigma}) &= \omega_\lambda^{-1/2}(\Theta_{\mathbf{k}\sigma}-\Theta^\dagger_{-\mathbf{k}\sigma}) \end{aligned}$$

Since the commutation relations of $\Xi's$ are identical to those of $a's$, and similarly for $\Theta's$ and $b's$, we can simplify notation by substituting $\Xi_{\mathbf{k}\sigma} \to a_{\mathbf{k}\sigma}$ and $\Theta_{\mathbf{k}\sigma} \to b_{\mathbf{k}\sigma}$. Thus,

$$\begin{aligned} H_2 = \frac{\hbar}{4}\sum_{\mathbf{k}\sigma}[&-(b_{-\mathbf{k}\sigma} - b^\dagger_{\mathbf{k}\sigma})(b_{\mathbf{k}\sigma} - b^\dagger_{-\mathbf{k}\sigma}) \\ &+ \omega_\lambda^2\ (b_{\mathbf{k}\sigma} + b^\dagger_{-\mathbf{k}\sigma})(b_{-\mathbf{k}\sigma} + b^\dagger_{\mathbf{k}\sigma}) \\ &- (a_{-\mathbf{k}\sigma} - a^\dagger_{\mathbf{k}\sigma})(a_{\mathbf{k}\sigma} - a^\dagger_{-\mathbf{k}\sigma}) \\ &+ (\omega_p^2 + \omega_k^2)(a_{\mathbf{k}\sigma} + a^\dagger_{-\mathbf{k}\sigma})(a_{-\mathbf{k}\sigma} + a^\dagger_{\mathbf{k}\sigma}) \\ &+ i2\omega_p(b_{\mathbf{k}\sigma} - b^\dagger_{-\mathbf{k}\sigma})(a_{-\mathbf{k}\sigma} + a^\dagger_{\mathbf{k}\sigma})\,] \end{aligned} \tag{5}$$

In Step 2, we aim to find a canonical transformation to H_3 using the formula $H_3 = e^S H_2\, e^{-S}$. We will determine S by

$$\begin{aligned} S = &-\frac{i}{2}\sum_{\mathbf{k}\sigma}\frac{\omega_\lambda\,\omega_p}{\omega_\lambda - \omega_k}(b_{\mathbf{k}\sigma}a_{-\mathbf{k}\sigma} + b^\dagger_{-\mathbf{k}\sigma}a_{-\mathbf{k}\sigma} \\ &+ b^\dagger_{-\mathbf{k}\sigma}a^\dagger_{\mathbf{k}\sigma} + b_{\mathbf{k}\sigma}a^\dagger_{\mathbf{k}\sigma}) \end{aligned}$$

$$\begin{aligned} H_3 &= e^S H_2\, e^{-S} \\ &= \frac{\hbar}{4}\sum_{\mathbf{k}\sigma}[-(b_{-\mathbf{k}\sigma} - b^\dagger_{\mathbf{k}\sigma})(b_{\mathbf{k}\sigma} - b^\dagger_{-\mathbf{k}\sigma}) \\ &\quad + \omega_B^2\ (b_{\mathbf{k}\sigma} + b^\dagger_{-\mathbf{k}\sigma})(b_{-\mathbf{k}\sigma} + b^\dagger_{\mathbf{k}\sigma}) \\ &\quad - (a_{-\mathbf{k}\sigma} - a^\dagger_{\mathbf{k}\sigma})(a_{\mathbf{k}\sigma} - a^\dagger_{-\mathbf{k}\sigma}) \\ &\quad + \omega_A^2(a_{\mathbf{k}\sigma} + a^\dagger_{-\mathbf{k}\sigma})(a_{-\mathbf{k}\sigma} + a^\dagger_{\mathbf{k}\sigma}) \\ &\quad - i\frac{2\,\omega_k\,\omega_p}{\omega_\lambda - \omega_k}(b_{\mathbf{k}\sigma} - b^\dagger_{-\mathbf{k}\sigma})(a_{-\mathbf{k}\sigma} + a^\dagger_{\mathbf{k}\sigma}) \\ &\quad - i\frac{2\,\omega_\lambda\,\omega_p}{\omega_\lambda - \omega_k}(b_{-\mathbf{k}\sigma} + b^\dagger_{\mathbf{k}\sigma})(a_{\mathbf{k}\sigma} - a^\dagger_{-\mathbf{k}\sigma})\,] \end{aligned} \tag{6}$$

As mentioned in the previous section, the photon with mode $\hbar\mathbf{k}_\lambda$ and $\hbar\omega_\lambda$ has already been annihilated, Therefore, in the above equations, the summation over $\mathbf{k}$ should exclude $\mathbf{k}_\lambda$, as it would lead to $\omega_k = \omega_\lambda$, causing the denominator to be zero and resulting in a singularity. This rule also applies to similar situations throughout this paper. Where

$$\omega_A^2 = \omega_k^2[1 + \frac{\omega_p^2}{(\omega_\lambda - \omega_k)^2}], \quad \omega_B^2 = \omega_\lambda^2[1 + \frac{\omega_p^2}{(\omega_\lambda - \omega_k)^2}]$$

In the third step, we apply the scale transformation described in Step 1 to the Hamiltonian H_3, resulting in H_4. A scale transformation, analogous to the one performed earlier, is then applied to H_3

$$\begin{aligned} (a_{\mathbf{k}\sigma} + a^\dagger_{-\mathbf{k}\sigma}) &= \omega_A^{-1/2}(\Xi_{\mathbf{k}\sigma} + \Xi^\dagger_{-\mathbf{k}\sigma}) \\ (a_{\mathbf{k}\sigma} - a^\dagger_{-\mathbf{k}\sigma}) &= \omega_A^{1/2}(\Xi_{\mathbf{k}\sigma} - \Xi^\dagger_{-\mathbf{k}\sigma}) \\ (b_{\mathbf{k}\sigma} + b^\dagger_{-\mathbf{k}\sigma}) &= \omega_B^{-1/2}(\Theta_{\mathbf{k}\sigma} + \Theta^\dagger_{-\mathbf{k}\sigma}) \\ (b_{\mathbf{k}\sigma} - b^\dagger_{-\mathbf{k}\sigma}) &= \omega_B^{1/2}(\Theta_{\mathbf{k}\sigma} - \Theta^\dagger_{-\mathbf{k}\sigma}) \end{aligned}$$

therefore

$$\begin{aligned} H_4 = \frac{\hbar}{4}\sum_{\mathbf{k}\sigma}\{&\omega_B[-(b_{-\mathbf{k}\sigma} - b^\dagger_{\mathbf{k}\sigma})(b_{\mathbf{k}\sigma} - b^\dagger_{-\mathbf{k}\sigma}) \\ &+\ (b_{\mathbf{k}\sigma} + b^\dagger_{-\mathbf{k}\sigma})(b_{-\mathbf{k}\sigma} + b^\dagger_{\mathbf{k}\sigma})] \\ &+ \omega_A[-(a_{-\mathbf{k}\sigma} - a^\dagger_{\mathbf{k}\sigma})(a_{\mathbf{k}\sigma} - a^\dagger_{-\mathbf{k}\sigma}) \\ &+ (a_{\mathbf{k}\sigma} + a^\dagger_{-\mathbf{k}\sigma})(a_{-\mathbf{k}\sigma} + a^\dagger_{\mathbf{k}\sigma})] \\ &- i\frac{2\omega_p\sqrt{\omega_\lambda\,\omega_k}}{\omega_\lambda - \omega_k}[(b_{\mathbf{k}\sigma} - b^\dagger_{-\mathbf{k}\sigma})(a_{-\mathbf{k}\sigma} + a^\dagger_{\mathbf{k}\sigma}) \\ &+ (b_{-\mathbf{k}\sigma} + b^\dagger_{\mathbf{k}\sigma})(a_{\mathbf{k}\sigma} - a^\dagger_{-\mathbf{k}\sigma})]\} \\ = \sum_{\mathbf{k}\sigma}[&\hbar\omega_B(b^\dagger_{\mathbf{k}\sigma}b_{\mathbf{k}\sigma} + \frac{1}{2}) + \hbar\omega_A(a^\dagger_{\mathbf{k}\sigma}a_{\mathbf{k}\sigma} + \frac{1}{2}) \\ &- i\frac{\hbar\omega_p\sqrt{\omega_\lambda\,\omega_k}}{\omega_\lambda - \omega_k}(b_{\mathbf{k}\sigma}a_{-\mathbf{k}\sigma} - b^\dagger_{-\mathbf{k}\sigma}a^\dagger_{\mathbf{k}\sigma})] \end{aligned} \tag{7}$$

In the fourth step, Bogoliubov transformations are applied to the Hamiltonian H_4. We introduce two new complex bosonic operators $\boldsymbol{\alpha}_{\mathbf{k}\sigma}$ and $\boldsymbol{\beta}_{\mathbf{k}\sigma}$, representing the new α and β elementary excitations, respectively. These operators are defined as:

$$\boldsymbol{\alpha}_{\mathbf{k}\sigma} \equiv c_1 b_{\mathbf{k}\sigma} + ic_2 a^\dagger_{-\mathbf{k}\sigma}, \tag{8}$$

$$\boldsymbol{\beta}_{\mathbf{k}\sigma} \equiv c_1 a_{\mathbf{k}\sigma} + ic_2 b^\dagger_{-\mathbf{k}\sigma}, \tag{9}$$

$$\begin{aligned} c_1^2 &= \frac{1}{2}\left[1 + \frac{(\omega_\lambda + \omega_k)I_1}{|\omega_\lambda - \omega_k|I_2}\right], \\ c_2^2 &= \frac{1}{2}\left[-1 + \frac{(\omega_\lambda + \omega_k)I_1}{|\omega_\lambda - \omega_k|I_2}\right], \\ I_1 &= \sqrt{(\omega_\lambda - \omega_k)^2 + \omega_p^2} = \sqrt{(\omega_\lambda - vk)^2 + \omega_p^2}, \\ I_2 &= \sqrt{(\omega_\lambda + \omega_k)^2 + \omega_p^2} = \sqrt{(\omega_\lambda + vk)^2 + \omega_p^2} \end{aligned}$$

where v denotes the speed of the bare photons that constitute the α and β elementary excitations. The commutation relations satisfied by the operators $\boldsymbol{\alpha}_{\mathbf{k}\sigma}$ and $\boldsymbol{\beta}_{\mathbf{k}\sigma}$ are given by: $[\boldsymbol{\alpha}_{\mathbf{k}\sigma}, \boldsymbol{\alpha}^\dagger_{\mathbf{k}'\sigma'}] = \delta_{\mathbf{k}\mathbf{k}'}\delta_{\sigma\sigma'}$, $[\boldsymbol{\beta}_{\mathbf{k}\sigma}, \boldsymbol{\beta}^\dagger_{\mathbf{k}'\sigma'}] = \delta_{\mathbf{k}\mathbf{k}'}\delta_{\sigma\sigma'}$, $[\boldsymbol{\alpha}_{\mathbf{k}\sigma}, \boldsymbol{\alpha}_{\mathbf{k}'\sigma'}] = [\boldsymbol{\alpha}_{\mathbf{k}\sigma}, \boldsymbol{\beta}_{\mathbf{k}'\sigma'}] = [\boldsymbol{\alpha}_{\mathbf{k}\sigma}, \boldsymbol{\beta}^\dagger_{\mathbf{k}'\sigma'}] = [\boldsymbol{\beta}_{\mathbf{k}\sigma}, \boldsymbol{\beta}_{\mathbf{k}'\sigma'}] = 0$. Hance, the final diagonlized Hamiltonian H_f is

$$H_f = \sum_{\mathbf{k}\sigma}\left[\hbar\omega_\alpha(\boldsymbol{\alpha}^\dagger_{\mathbf{k}\sigma}\boldsymbol{\alpha}_{\mathbf{k}\sigma} + 1/2) + \hbar\omega_\beta(\boldsymbol{\beta}^\dagger_{\mathbf{k}\sigma}\boldsymbol{\beta}_{\mathbf{k}\sigma} + 1/2)\right] \tag{10}$$

$$\hbar\omega_\alpha = (\hbar/2)(I_2 + I_1) \tag{11}$$

$$\hbar\omega_\beta = (\hbar/2)(I_2 - I_1) \tag{12}$$

Therefore, the exact eigenvalues $E_{n_{\alpha_{\mathbf{k}\sigma}} n_{\beta_{\mathbf{k}\sigma}}}$ and Fock states $|n_{\alpha_{\mathbf{k}\sigma}} n_{\beta_{\mathbf{k}\sigma}}\rangle$ for H_f are as follows:

$$E_{n_{\alpha_{\mathbf{k}\sigma}} n_{\beta_{\mathbf{k}\sigma}}} = \hbar\omega_\alpha(n_{\alpha_{\mathbf{k}\sigma}} + 1/2) + \hbar\omega_\beta(n_{\beta_{\mathbf{k}\sigma}} + 1/2) \tag{13}$$

$$|n_{\alpha_{\mathbf{k}\sigma}}\rangle = \frac{(\boldsymbol{\alpha}^\dagger_{\mathbf{k}\sigma})^{n_{\alpha_{\mathbf{k}\sigma}}}}{\sqrt{n_{\alpha_{\mathbf{k}\sigma}}!}}\,|0\rangle\,, |n_{\beta_{\mathbf{k}\sigma}}\rangle = \frac{(\boldsymbol{\beta}^\dagger_{\mathbf{k}\sigma})^{n_{\beta_{\mathbf{k}\sigma}}}}{\sqrt{n_{\beta_{\mathbf{k}\sigma}}!}}\,|0\rangle \tag{14}$$

$$|n_{\alpha_{\mathbf{k}\sigma}} n_{\beta_{\mathbf{k}\sigma}}\rangle = |n_{\alpha_{\mathbf{k}\sigma}}\rangle \otimes |n_{\beta_{\mathbf{k}\sigma}}\rangle\,, n_{\alpha_{\mathbf{k}\sigma}}, n_{\beta_{\mathbf{k}\sigma}} = 0, 1, 2, ... \tag{15}$$

Mathematically, H is identical to Hopfield's Hamiltonian[9]. However, the eigenfunctions we obtained, as shown in Equation (15), are a new set of α and β elementary excitations formed by the coupling of a DP and bare photons, which are completely different from his.

From Equations (11) or (12), it can be seen that the α and β elementary excitations have their respective spectral ranges: $0 \leqslant \omega_\beta(k) < \omega_\lambda, \omega_\alpha(k) \geqslant \omega_d$, where $\omega_d^2 \equiv \omega_\lambda^2 + \omega_p^2$. Therefore, does $\omega_\lambda < \omega < \omega_d$ correspond to the energy gap? If not, what is the relationship between these energy states and the α and β elementary excitations?

To address this, we first determine the wave vector of an elementary excitation based on Equations (11) or (12):

$$k^2 = \frac{\omega^2(\omega^2 - \omega_d^2)}{v^2(\omega^2 - \omega_\lambda^2)} \tag{16}$$

When $\omega_\lambda < \omega < \omega_d$, the wave vector k becomes imaginary. This indicates that the energy states within this spectral range are unstable. Substituting an imaginary wave vector ik into Equations (11) and (12), we find that $\hbar\omega_\beta(ik)$ is imaginary and can be neglected. The remaining term, $\hbar\omega_\alpha(ik)$, is real, and it is defined as $\hbar\omega_\gamma(k)$, i.e., $\hbar\omega_\gamma(k) \equiv \hbar\omega_\alpha(ik)$, and is given by:

$$\begin{aligned}
&\hbar\omega_\gamma(k) \\
&= \frac{\hbar}{2}\left(\sqrt{(\omega_\lambda + iv_\gamma k)^2 + \omega_p^2} + \sqrt{(\omega_\lambda - iv_\gamma k)^2 + \omega_p^2}\right) \\
&= \frac{\hbar}{\sqrt{2}}\left(\omega_d^2 - v_\gamma^2 k^2 + \sqrt{\left(\omega_d^2 - v_\gamma^2 k^2\right)^2 + 4v_\gamma^2 k^2 \omega_\lambda^2}\right)^{1/2}
\end{aligned} \tag{17}$$

The corresponding energy states are referred to as γ elementary excitations. Alternatively, the γ elementary excitation can be seen as the α elementary excitation with an imaginary wave vector. Here, v_γ denotes the speed of the bare photon that contributes to the formation of the γ elementary excitation. In summary, $\omega_\beta(k)$, $\omega_\gamma(k)$ and $\omega_\alpha(k)$ have their respective spectral ranges: $0 \leqslant \omega_\beta(k) < \omega_\lambda$, $\omega_\lambda < \omega_\gamma(k) \leqslant \omega_d$ and $\omega_\alpha(k) \geqslant \omega_d$.

Additionally, not only will we observe from Fig. 3 that the dispersion relations $\omega_\beta(k)$ and $\omega_\alpha(k)$ are very similar to the dispersion relation of a bare photon. Therefore, we uniformly refer to these elementary excitations as physicalized photons (PP), which can be considered photons with nonzero rest mass. To highlight their connection to the λ transition point, the α, β and γ elementary excitations are respectively referred to as $\alpha(\lambda)$ PP, $\beta(\lambda)$ PP, and $\gamma(\lambda)$ PP. The abbreviation is λ-PP.

III. KEY CHARACTERISTICS OF THE α, β AND γ PP

The definitions of $\boldsymbol{\alpha}_{\mathbf{k}\sigma}$ and $\boldsymbol{\beta}_{\mathbf{k}\sigma}$ PPs in Equations (8) and (9) provide a formal mathematical description, but their physical interpretation remains elusive. To gain a clearer understanding of their nature and their connection to DP and BBR, the corresponding canonical coordinates $Q_\alpha(\mathbf{k},\sigma)$, $Q_\beta(\mathbf{k},\sigma)$ and momenta $\Pi_\alpha(\mathbf{k},\sigma)$, $\Pi_\beta(\mathbf{k},\sigma)$ are given by

$$\begin{aligned}
Q_\alpha(\mathbf{k},\sigma) =& \left(\frac{\hbar}{2m\omega_\alpha}\right)^{1/2}(\boldsymbol{\alpha}_{\mathbf{k}\sigma} + \boldsymbol{\alpha}^\dagger_{-\mathbf{k}\sigma}) \\
=& c_1\sqrt{\frac{\omega_\lambda}{\omega_\alpha}}\,B(\mathbf{k},\sigma) + \frac{c_2}{\sqrt{mm_p\omega_\alpha\omega_k}}\,\Pi_A(\mathbf{k},\sigma) \\
\Pi_\alpha(\mathbf{k},\sigma) =& -i\left(\frac{\hbar m\omega_\alpha}{2}\right)^{1/2}(\boldsymbol{\alpha}_{\mathbf{k}\sigma} - \boldsymbol{\alpha}^\dagger_{-\mathbf{k}\sigma}) \\
=& c_1\sqrt{\frac{\omega_\alpha}{\omega_\lambda}}\,\Pi_B(\mathbf{k},\sigma) + c_2\sqrt{mm_p\omega_\alpha\omega_k}\,A(\mathbf{k},\sigma) \\
Q_\beta(\mathbf{k},\sigma) =& \left(\frac{\hbar}{2m\omega_\beta}\right)^{1/2}(\boldsymbol{\beta}_{\mathbf{k}\sigma} + \boldsymbol{\beta}^\dagger_{-\mathbf{k}\sigma}) \\
=& c_1\sqrt{\frac{m_p\omega_k}{m\omega_\beta}}\,A(\mathbf{k},\sigma) + \frac{c_2}{\sqrt{m^2\omega_\beta\omega_\lambda}}\,\Pi_B(\mathbf{k},\sigma) \\
\Pi_\beta(\mathbf{k},\sigma) =& -i\left(\frac{\hbar m\omega_\beta}{2}\right)^{1/2}(\boldsymbol{\beta}_{\mathbf{k}\sigma} - \boldsymbol{\beta}^\dagger_{-\mathbf{k}\sigma}) \\
=& c_1\sqrt{\frac{m\omega_\beta}{m_p\omega_k}}\,\Pi_A(\mathbf{k},\sigma) + c_2\sqrt{m^2\omega_\beta\omega_\lambda}\,B(\mathbf{k},\sigma)
\end{aligned} \tag{18}$$

And we have $[Q_\alpha(\mathbf{k},\sigma), \Pi_\alpha(-\mathbf{k}',\sigma')] = i\hbar\delta_{\mathbf{k}\mathbf{k}'}\delta_{\sigma\sigma'}$, $[Q_\beta(\mathbf{k},\sigma), \Pi_\beta(-\mathbf{k}',\sigma')] = i\hbar\delta_{\mathbf{k}\mathbf{k}'}\delta_{\sigma\sigma'}$. Interestingly, the canonical coordinates and momenta of $\alpha(\lambda)$ and $\beta(\lambda)$ PPs exhibit a chimeric nature, being crossed linear combinations of DP and BBR components. It is precisely the photon components contained in the PPs that provide the physical reason for the possible superfluidity of the PPs.

We note that the spectrum of bare photons ω_k (excluding ω_λ) corresponding to T_λ was used when deriving $\omega_\alpha(k)$, $\omega_\beta(k)$ and $\omega_\gamma(k)$, which are implicitly temperature dependent. To explicitly show this dependence, we use the notation $\omega_\alpha(T_\lambda,k)$, $\omega_\beta(T_\lambda,k)$, and $\omega_\gamma(T_\lambda,k)$. How do these frequencies change when the temperature changes from T_λ to T? For the Planck distribution of bare photons, we have a scaling relation between T_1 and its spectrum $\omega(T_1,k)$, and T_2 and its spectrum $\omega(T_2,k)$: $\omega(T_1,k)/T_1 = \omega(T_2,k)/T_2$. Assuming a similar scaling relations for PPs, we obtain:

$$\begin{aligned}
\omega_\beta(T,k) &= (T/T_\lambda)\,\omega_\beta(T_\lambda,k) \\
\omega_\gamma(T,k) &= (T/T_\lambda)\,\omega_\gamma(T_\lambda,k) \\
\omega_\alpha(T,k) &= (T/T_\lambda)\,\omega_\alpha(T_\lambda,k)
\end{aligned} \tag{19}$$

For $\beta(\lambda)$ PPs, since the variation of the wavevector $k \in [0,\infty)$ does not change the range of the spectrum, i.e., $0 \leqslant \omega_\beta(T,k) < \omega_\lambda$ and $0 \leqslant \omega_\beta(T_\lambda,k) < \omega_\lambda$, combined with equation (19), this implies that the $\beta(\lambda)$ PPs have their own temperature range: $\beta(\lambda)$ PPs: $0 \leqslant T < T_\lambda$. Similarly, $\alpha(\lambda)$ PPs: Imaginary wave vector part($\gamma(\lambda)$

PPs): $T_\lambda < T \leqslant T_{\lambda\,d}$, where $T_{\lambda\,d} \equiv (\omega_d/\omega_\lambda)T_\lambda$; Real wave vector part: $T \geqslant T_{\lambda\,d}$.

Using Equations (16) and (19), the density of state of λ-PPs $g(k)$ is

$$g(k) = \frac{2V}{h^3}4\pi\hbar^3k^2 = \frac{V\omega^2(T,k)}{\pi^2v^2}\,\frac{\omega^2(T,k)-\omega_d^2}{\omega^2(T,k)-\omega_\lambda^2} = \frac{Vb^2\omega^2(T_\lambda,k)}{\pi^2v^2}\,\frac{b^2\omega^2(T_\lambda,k)-\omega_d^2}{b^2\omega^2(T_\lambda,k)-\omega_\lambda^2} \tag{20}$$

where h is Planck constant, $\hbar = h/2\pi$, $b \equiv T/T_\lambda$. Depending on the temperature range, $\omega(T_\lambda,k)$ can be expressed as $\omega_\beta(T_\lambda,k)$, $\omega_\gamma(T_\lambda,k)$ or $\omega_\alpha(T_\lambda,k)$. In the case of λ-PPs, the density of states $g(k)$ tends to infinity only when $T \to T_\lambda$.

A long-standing question is: Why does ^{4}He exhibit singular specific heat at both the lambda point and the critical point, yet superfluidity only occurs at the lambda point? This question can be traced back to Landau[4] "critical velocity" criterion for superfluidity. The dispersion relations of transverse modes $\alpha(\lambda)$, $\gamma(\lambda)$, and $\beta(\lambda)$ of PPs are shown in Fig. 3. $\gamma(\lambda)$ and $\alpha(\lambda)$ PPs are formally the first and second excited bands of $\beta(\lambda)$ PP, respectively. According to Landau's criterion, Fig. 3 shows that only $\partial\,\omega_\beta(T,k)/\partial\,k > 0$ in the long-wavelength limit. This implies that only $\beta(\lambda)$ PPs might exhibit superfluidity. Our research indicates that Landau's condition is merely a necessary condition and needs further supplementation. As mentioned earlier in this paper, the interaction between ^{4}He atoms in DP and those outside DP leads to two consequences: 1. It makes each of the ^{4}He atoms in DP an isotropic harmonic oscillator, and the transverse sound velocity of PPs coincides with their longitudinal sound velocity, resulting in superfluidity, as observed in the superfluid transition at the lambda point; 2. It makes each of the ^{4}He atoms in DP an anisotropic harmonic oscillator, where the vibration frequency and sound velocity of the longitudinal mode differ from those of the transverse mode. If the interaction is not strong enough and only perturbs the ^{4}He atoms in λ-PPs, then λ-PPs cannot be in the eigenstates as described in Equation (15), but rather in a superposition of eigenstates, which is called a damped PP and no superfluidity is observed. Is there any relationship between the magnitude of the damping force and the formation of DP? We provide the corresponding classical scenario as a reference. Let c_1 be the damping coefficient, and $\zeta \equiv c_1/2m\omega_\lambda$ be the damping ratio. Then the resonant frequency is given by $\omega_r = \omega_\lambda\sqrt{1-2\zeta^2}$. The resonant frequency ω_r has a critical point at $\zeta = 1/\sqrt{2}$. When $\zeta > 1/\sqrt{2}$, DP should not appear, and neither should PP, and naturally, superfluidity will not appear. The non-superfluid transition at the critical point should belong to the second category with $\zeta < 1/\sqrt{2}$. Therefore, overall, there are two classes of PPs: lambda (λ) and critical (c). Each class has three types: α, β, and γ. Thus, there are six types of PPs: $\alpha(\lambda)$, $\beta(\lambda)$, $\gamma(\lambda)$, $\alpha(c)$, $\beta(c)$, and $\gamma(c)$. According to the superfluidity criterion mentioned above, $\beta(\lambda)$ is the only type of PP with superfluidity.

It's important to note that when heating or cooling liquid helium across the lambda point, T_λ, the microscopic structures on either side of T_λ are asymmetric. This asymmetry leads to a difference between the transition temperatures during heating, T_λ(heating), and cooling, T_λ(cooling). This difference is known as thermal hysteresis. Generally, the transition temperature T_λ is higher during heating than during cooling. This hysteresis is also observed at the critical point.

At this point, we can fully describe the physical process of ^{4}He at $T \leqslant T_\lambda$ (here, we only consider the cooling process through T_λ). When the density of ^{4}He is ρ_λ and the temperature drops to T_λ, the DP composed of N_λ ^{4}He atoms and bare photons form three possible λ-PPs according to Equation (18): $\beta(\lambda)$-PPs, $\gamma(\lambda)$-PPs, and $\alpha(\lambda)$-PPs. They each have their respective spectral ranges: $0 \leqslant \omega_\beta(k) < \omega_\lambda$, $\omega_\lambda < \omega_\gamma(k) \leqslant \omega_d$ and $\omega_\alpha(k) \geqslant \omega_d$. Since $k \in [0,\infty)$, this implies that all wavelengths of bare photons corresponding to T_λ are physicalized into λ-PPs, so we say that the temperature T_λ is physicalized. λ-PPs are referred to as physicalized temperature (PT), which is a subsystem with long-range periodic structure. The energy spectrum of this subsystem varies with temperature according to Equation (19), but its structure only changes at two temperatures, T_λ and $T_{\lambda d}$, according to Equation (18). Among these, only $\beta(\lambda)$-PPs may exhibit superfluidity. Similarly, at the critical point, T_c will also be physicalized, with the difference being the value of the parameters, and all three types of c-PPs do not exhibit superfluidity.

The following table lists the various components of the system at different temperature ranges. T_c, T_b, and T_λ represent the critical, boiling, and lambda temperatures, respectively, with values of 5.18 K, 4.22 K, and 2.17 K. N_c and N_L denote the number of ^{4}He atoms in the c-PP and normal liquid state, respectively. As the temperature decreases, N_c and N_L gradually decrease, while the number of atoms in the λ-PP, N_λ, increases. This trend is due to the energy hierarchy: c-PP > λ-PP. The properties of α-PP are very similar to those of bare photons and, therefore, are not listed separately in Table I.

IV. THE APPLICATIONS OF THE PT MODEL TO ^{4}He

A. On the Critical Opalescence

Based on Equations (16) and (19), the transverse dielectric function, ε_t(or equivalently, the index of refraction, n) can be determined.

$$n^2 = \varepsilon_t(\omega) \equiv \frac{k^2}{\omega^2} = \frac{1}{v^2}\,\frac{b^2\omega^2(T_\lambda,k)-\omega_d^2}{b^2\omega^2(T_\lambda,k)-\omega_\lambda^2} \tag{21}$$

When $T_\lambda < T \leqslant T_{\lambda\,d}$ or $T_c < T \leqslant T_{c\,d}$, $n^2 < 0$, which indicates strong light scattering by $\gamma(\lambda)$ PP or damped $\gamma(c)$

TABLE I. The composition of ^{4}He as a function of temperature.

Temperature range	Components	Notes
$[T_c, \infty)$	classical ideal gas ^{4}He	$(T_c, T_{c\,d}]$ γ(c) PPs while heating across T_c
$[T_b, T_c)$	β(c) PPs, gas ^{4}He	
$(T_\lambda, T_b]$	β(c) PPs, normal liquid ^{4}He	$(T_\lambda, T_{\lambda\,d}]$ $\gamma(\lambda)$ PPs while heating across T_λ
$[0, T_\lambda)$	β(c) and $\beta(\lambda)$ PPs, normal liquid ^{4}He	

PP and leading to a phenomenon known as opalescence. However, when $T_\lambda < T \leqslant T_{\lambda\,d}$, the $\gamma(\lambda)$ PP coexists with the damped $\beta(c)$ PP, which does not scatter light strongly. As a result, λ opalescence is nearly absent, and only critical opalescence is observed.

B. On the Specific Heat Across All Temperatures

One of the most important physical quantities for superfluid ^{4}He is a sharp, narrow, and singular peak in the specific heat at the so-called lambda point and critical point, T_λ and T_c. Based on the RG approach, the specific heat can be calculated closely near the transition point. However, far from T_c, the RG approach does not agree well with experimental data[6]. Moreover, the RG approach does not provide a physical mechanism to explain why the system fluctuates so strongly near the lambda and critical points. As for Landau's two-fluid model[2, 3], it does not predict any singularity in the specific heat. Based on the PT model, we will find that below T_λ, the specific heat is mainly contributed by $\beta(\lambda)$ PPs, while above T_λ, it is mainly contributed by $\gamma(\lambda)$ PPs. Similarly, below T_c, the specific heat is mainly contributed by $\beta(c)$ PPs, while above T_c, it is mainly contributed by $\gamma(c)$ PPs. This means that the physical mechanisms underlying the specific heat on either side of the singularity are different. It is therefore inappropriate to fit the data with a single logarithmic or power-law function, which exhibits a singularity.

The specific heat of the PPs at constant volume can be described by the following equation:

$$C_v = k_B \int_0^\infty \left(\frac{\hbar\omega}{2k_BT}\right)^2 \operatorname{csch}^2\left(\frac{\hbar\omega}{2k_BT}\right) g(k)\mathrm{d}k \quad (22)$$

Where k_B is the Boltzmann constant. Using Equation (20) and temperature as the energy unit, the specific heat of λ PPs can be calculated with three temperature intervals:

$$\begin{aligned}
C_{v\beta}(T) &= \frac{C_\lambda}{v^2T^2}\int_0^\infty \mathrm{S}(b\,\omega_\beta)\,\mathrm{d}k, \qquad T \in [0, T_\lambda)\\
C_{v\gamma}(T) &= \frac{C_\lambda}{v_\gamma^2T^2}\int_\infty^0 \mathrm{S}(b\,\omega_\gamma)\,\mathrm{d}k, \qquad T \in (T_\lambda, T_{\lambda\,d}]\\
C_{v\alpha}(T) &= \frac{C_\lambda}{v^2T^2}\int_0^\infty \mathrm{S}(b\,\omega_\alpha)\,\mathrm{d}k, \qquad T \in [T_{\lambda\,d}, \infty)\\
\mathrm{S}(\omega) &\equiv \frac{\omega^2(T,k)-\omega_d^2}{\omega^2(T,k)-\omega_\lambda^2}\;\omega^4(T,k)\operatorname{csch}^2(\omega(T,k)/2T).
\end{aligned} \quad (23)$$

where $C_\lambda \equiv R/(4\pi^2\rho_{s\lambda})$, $R = k_BN_A$ is the molar gas constant, where N_A is the Avogadro constant. $\rho_{s\lambda} \equiv N_\lambda/V$ is the density of superfluid, which should vary with temperature but is not predicted by the PT model and must be obtained experimentally. Here, it is treated as a constant because the experimental data for specific heat includes contributions from both the superfluid and non-superfluid components, so this constant represents the portion contributed by the superfluid component. For the damped c PPs, one can substitute the parameters for T_c into Equation (23) to obtain a different set of C_v values. There are six types of PPs that contribute to the specific heat: $\alpha(\lambda)$, $\beta(\lambda)$, $\gamma(\lambda)$, $\alpha(c)$, $\beta(c)$ and $\gamma(c)$ PP. Since each PP is independent of one another, the specific heat for any given temperature is the superposition of the two where the temperatures overlap as shown in Fig. 1. According to the Dulong-Petit law, $C_v = 3R/2$ when $T > T_c$.

C. On Landau's Phonon-Roton Dispersion Relation

When calculating C_v values, we used six dispersion relations from two types of PPs: λ-PP and c-PP. None of these dispersion relations match the P-R curve predicted by Landau[3]. Since then, numerous complex theoretical models, such as Feynman's model[12, 13], have been proposed to calculate it, but they show significant discrepancies with experimental results. Moreover, hundreds of papers have been referenced in Glyde[14] and Godfrin's[15] survey of superfluid ^{4}He papers. Despite these efforts, the physical picture of the roton remains ambiguous. Since the P-R curve is obtained from neutron inelastic scattering experiments, we will analyze the experimental processes and data using the PT model.

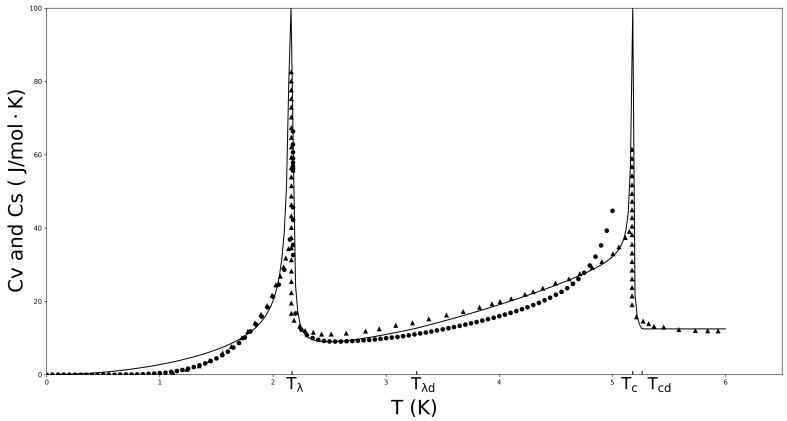

FIG. 1. Temperature dependence of the specific heat of ^{4}He. Circles[10] represent experimental data of the specific heat at saturated vapor pressure; triangles[11] represent data at constant volume; the solid line is the calculated result from this work. $\rho_{s\lambda}$, ρ_{sc} and the parameters of the spectra used in the calculations are as follows: for the λ point, $\rho_{s\lambda} = 0.00736$ g/cm^3 (as a reference, the experimental value[10] of the density of superfluid ^{4}He at 2.17 K is 0.00729 g/cm^3), $\hbar\omega_\lambda = 39\,\mathrm{K}$, $\hbar\omega_p = 44\,\mathrm{K}$, $v = 61.5\,\mathrm{K\AA} = 805.2$ m/s , $v_\gamma = 120\,\mathrm{K\AA}$= 1571.1 m/s; for the critical point, $\rho_{sc} = 0.00364$ g/cm^3 (no experimental data is available for reference), $\hbar\omega_c = 100\,\mathrm{K}$, $\hbar\omega_p = 18\,\mathrm{K}$, $v = 61.5\,\mathrm{K\AA} = 805.2$ m/s , $v_\gamma = 90\,\mathrm{K\AA}$= 1178.3 m/s.

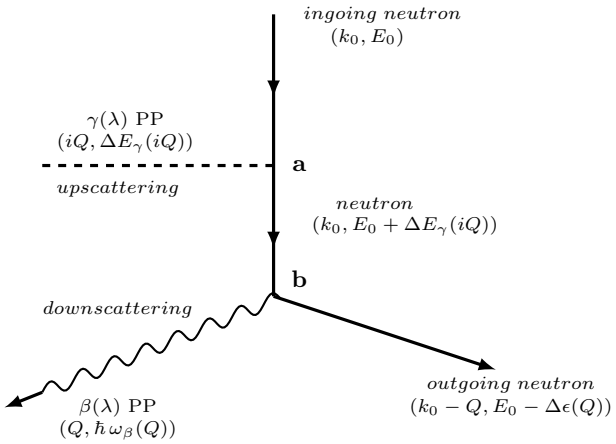

FIG. 2. Schematic diagram of inelastic scattering processes between a neutron and $\gamma(\lambda)$, $\beta(\lambda)$ PPs.

The kinematics of neutron scattering are illustrated in Fig. 2. Initially, an incident neutron has initial energy E_0 and momentum k_0. Before exiting, it undergoes two scatterings. At (a) in Fig. 2, it upscatters with an unstable $\gamma(\lambda)$ PP. The $\gamma(\lambda)$ PP has excitation energy $\Delta E_\gamma(iQ) = \hbar\omega_\gamma(Q_0 - Q) - \hbar\omega_\lambda$, where $\hbar\omega_\lambda$ is the ground state energy of the γ PP, and Q_0 is determined by $\hbar\omega_\gamma(Q_0) = \hbar\omega_\lambda$. After (a), the incident neutron energy becomes $E_0 + \Delta E_\gamma(iQ)$, with no change in its momentum due to the imaginary momentum of the γ PP. Following this, at (b) in Fig. 2, the neutron downscatters with a stable $\beta(\lambda)$ PP. The $\beta(\lambda)$ PP gains momentum Q with energy $\hbar\omega_\beta(Q)$. Therefore, the final transferred energy of the outgoing neutron $\Delta\varepsilon(Q) = E_0 - [E_0 + \Delta E_\gamma(iQ) - \hbar\omega_\beta(Q)] = \hbar\omega_\beta(Q) - [\hbar\omega_\gamma(Q_0 - Q) - \hbar\omega_\lambda]$. The final momentum of the outgoing neutron is $k_0 - (k_0 - Q) = Q$. When we substitute parameters from the caption of Fig. 1, we obtain Fig. 3. The curve $\Delta\varepsilon(Q) \sim Q$ is precisely the P-R curve. Hence, we can conclude that there is no such thing as a roton[3], and the P-R curve cannot even be called a dispersion relation because it does not correspond to the spectrum of a single quasiparticle. The P-R curve is merely a spurious effect caused by neutron inelastic scattering.

For the damped c-PPs, there is also a P-R curve-like feature. However, the damped c-PP is in a non-eigenstate, so many P-R curve-like features with different energies coexist. As the energy of the c-PPs is greater than that of the λ PPs, it leads to the formation of a broad diffuse background above the P-R curve in Fig. 3. These are simply the results of experiments[16–18].

D. On the Quantization of Circulation and Magnetic Fluxes

Similar to Vinen's experiment [19], an experiment based on the PT model for measuring superfluid ^{4}He circulation is shown in the schematic in Fig. 4. When a cylindrical container of He II is rotated about its axis at an angular velocity exceeding a small critical value, Ω_{c1}, we propose a departure from conventional understanding: the liquid helium separates into three distinct phases. The non-superfluid components (normal fluid + $\beta(c)$ PPs) migrate to the container walls and bottom or to the wire surface, forming a uniformly porous parabolic liquid surface. These components arrange themselves into an array of vortex-annulated columns parallel to the rotation axis.

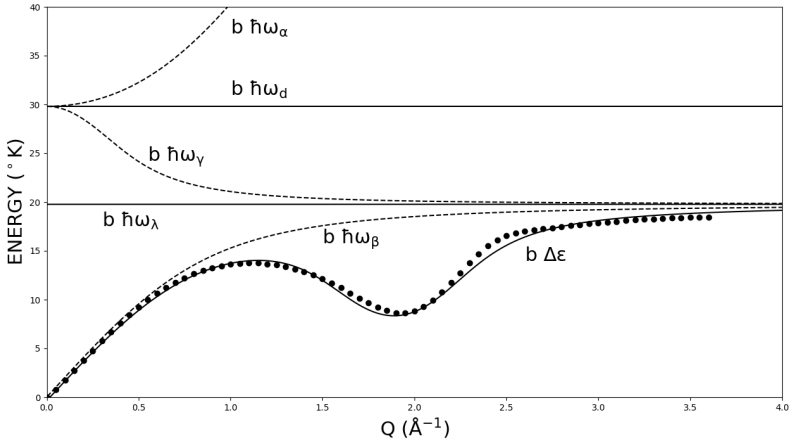

FIG. 3. Shows the dispersion curves of $b\,\alpha(\lambda)$, $b\,\gamma(\lambda)$, $b\,\beta(\lambda)$ PPs, the P-R curve $b\,\Delta\varepsilon(Q)$ along with experimental data[10, 16] obtained from inelastic neutron scattering at a temperature of $T_{\rm exp}$=1.1 K. The parameters used here are the same as those in Fig. 1. The wavevector Q_0 is determined by the condition $\hbar\omega_\gamma(Q_0) = \hbar\omega_\lambda$, yielding a value of $Q_0 \approx 1.91\text{Å}^{-1}$. The reduced temperature b is defined as the ratio of the experimental temperature to the lambda temperature, i.e., $b = T_{\rm exp}/T_\lambda = 1.1/2.17$.

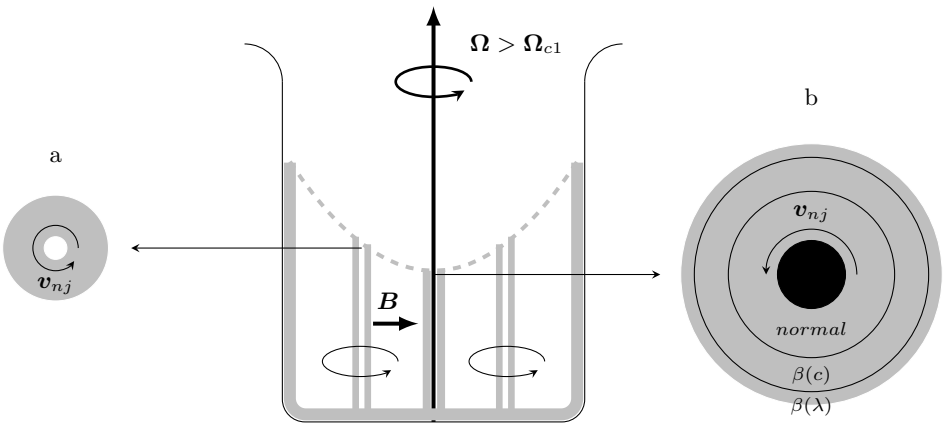

FIG. 4. Schematic diagram of an experiment similar to Vinen's experiment[19]. A constant magnetic field, $\boldsymbol{B}$, is applied. (a) Cross-sectional view of the annulus transition region. (b) Cross-sectional view of the cylindrical wire and transition region. The exaggerated dimensions of this cross-section are used to clearly show the details of the composition and structure of the gray region: near the surface of the wire is normal fluid ^{4}He, and the thickness of a thin layer near the outer surface of the gray region represents the penetration depth of the superfluid component, $\beta(\lambda)$ PPs. The middle layer is mainly composed of damped $\beta(c)$ PPs. The two inner layers are both non-superfluid. Other gray regions in this figure can be understood similarly. The microstructures of the transition region closely resemble the response of a Type-II superconductor to a magnetic field, known as the mixed state. In Vinen's experiment[19], there are only two components: normal fluid and superfluid, and no phase separation occurs, so there are no gray regions.

The non-superfluid helium is thus enclosed by the superfluid component. Transition regions exist where the superfluid penetrates into the non-superfluid, leading to a solid-body-like rotation of He II. At sufficiently high angular velocities, Ω_{c2}, the superfluid reverts to the normal state[20].

The wire would experience a Magnus force, which is a function of the entire transition region, rather than being solely dependent on the normal fluid immediately adjacent to the wire surface. Let $\boldsymbol{v}_{nj}$ and $\boldsymbol{v}_{sj}$ denote the velocity of jth ^{4}He atom of the normal fluid and superfluid, respectively. Since the the mechanical momentum $m\boldsymbol{v}_{nj}$ equals the canonical momentum $\boldsymbol{P}_{nj}$, applying the Bohr-Sommerfeld quantization condition, the circulation of the normal fluid ^{4}He around any circuit in the transition region is: $\oint_\ell \boldsymbol{v}_{nj}\cdot \mathrm{d}\boldsymbol{r}_j = \frac{1}{m}\oint_\ell \boldsymbol{P}_{nj}\cdot \mathrm{d}\boldsymbol{r}_j = n(h/m),\ \ n = 0, \pm1, \pm2, \cdots$. It implies that the circulation of normal fluid ^{4}He is quantized in units of h/m. In the special case of Fig. 4(a), due to the limitation imposed by the Heisenberg uncertainty principle, the case where $n = 0$ in nh/m should be excluded. This is why the cross-sectional diagram is hollow. Experimental ob-

servations have confirmed this phenomenon at the levels of one, two, and three quantum units[21]. However, when considering the contributions of the transition region, the quantization of the circulation's average value easily breaks down. This finding aligns with Vinen's experimental observations[19]. Another point worth noting is that the Bohr-Sommerfeld quantization condition arises from the wave nature of particles; therefore, the quantization of the circulation of normal fluid ^{4}He arises from the wave nature of ^{4}He rather than its superfluidity.

According to Equation (3), the mechanical momentum $m\boldsymbol{v}_{sj}$ includes both the canonical momentum $\boldsymbol{P}_{sj}$ and the electromagnetic momentum $\eta\boldsymbol{A}_j$. Landau[2] postulated that the $\boldsymbol{v}_{sj}$ satisfies the condition $\nabla\times\boldsymbol{v}_{sj}=0$. Therefore, the circulation of the superfluid is: $\oint_\ell \boldsymbol{v}_{sj}\cdot\mathrm{d}\boldsymbol{r}_j = \frac{1}{m}\oint_\ell(\boldsymbol{P}_{sj}-\eta\boldsymbol{A}_j)\cdot\mathrm{d}\boldsymbol{r}_j$. Using Landau's postulation and the Bohr-Sommerfeld quantization condition $\oint_\ell \boldsymbol{v}_{sj}\cdot\mathrm{d}\boldsymbol{r}_j = \iint_s(\nabla\times\boldsymbol{v}_{sj})\cdot\mathrm{d}\boldsymbol{s}=0$. $\oint_\ell \boldsymbol{P}_{sj}\cdot\mathrm{d}\boldsymbol{r}_j = nh,\ n=0,\pm1,\pm2,\cdots$. and $\oint_\ell \eta\boldsymbol{A}_j\cdot\mathrm{d}\boldsymbol{r}_j = \eta\iint_s(\nabla\times\boldsymbol{A}_j)\cdot\mathrm{d}\boldsymbol{s}=\eta\Phi$. where Φ is the magnetic flux passing through curl surface S. Combining these equations, we obtain $\Phi=n\Phi_0$, which is quantization of magnetic flux. Φ_0 is the quantum of flux, given by h/η. We propose an experiment to test this result. A constant magnetic field is applied parallel to the rotational axis of a rotating torus container filled with superfluid ^{4}He. The experiment aims to observe whether the magnetic flux, as a function of angular velocity, is quantized. Additionally, the coupling constant η can be measured through this experiment. In summary, according to our PT model, there are two types of quantization: the circulation of normal fluid ^{4}He is quantized in units of h/m, while the circulation of superfluid ^{4}He is identically zero. However, this latter condition leads to quantization of the magnetic flux in units of h/η.

For comparison, the Landau two-fluid model[2, 3] neither includes the phase separation between the superfluid and normal fluid nor the quantization of magnetic flux. It merely states that when the integration circuit in $\oint_\ell \boldsymbol{v}_{sj}\cdot\mathrm{d}\boldsymbol{r}_j$ encloses the axis of the vortex, $\oint_\ell \boldsymbol{v}_{sj}\cdot\mathrm{d}\boldsymbol{r}_j = nh/m$, otherwise $\oint_\ell \boldsymbol{v}_{sj}\cdot\mathrm{d}\boldsymbol{r}_j = 0$. As for the reason why this same integral gives different results in these cases, the theory attributes it to the singularity at the center of the vortex line. However, the theory does not explain the physical mechanism behind this singularity. These conclusions do not account for two important physical facts: 1. the mechanical momenta of superfluid and normal fluid ^{4}He atoms are inherently different; 2. in normal fluid ^{4}He, the motion of ^{4}He atoms reflects single-particle behavior, whereas the quasiparticle $\beta(\lambda)$ PP reflects the coherent behavior of N_λ ^{4}He atoms.

V. CONCLUSIONS

We propose the following unique assumption: when photons interact with atoms (or matter), under certain conditions, not only can phonons generate photons through energy changes, but the reverse process is also possible, meaning that derivative phonons (DP) can appear. Through the coupling between DP and bare photons, a new Bose-type elementary excitation—Physicalized photon (PP)—is formed. When all bare photons of wavelength at a temperature T_λ become quasiparticle PPs, we say that the temperature T_λ has been Physicalized. The so-called physical picture of N_λ superfluid ^{4}He atoms is as follows: N_λ ^{4}He atoms with dressed photons (i.e., PT), although subjected to the damped effects of non-superfluid helium atoms, still move like photons as long as the damping ratio $\zeta < 1/\sqrt{2}$, meaning they exhibit superfluidity.

[1] L. Tisza, Nature **141**, 913 (1938).
[2] L. D. Landau, J. Phys. USSR **5**, 71 (1941).
[3] L. D. Landau, J. Phys. USSR **11**, 91 (1947).
[4] K. G. Wilson, Phys. Rev. B **4**, 3174 (1971).
[5] K. G. Wilson, Phys. Rev. B **4**, 3184 (1971).
[6] H. E. Stanley, Rev. Mod. Phys. **71**, S358 (1999).
[7] P. A. M. Dirac, Proc. Roy. Soc. A **114**, 243 (1927).
[8] L. I. Schiff, *Quantum Mechanics* (McGraw-Hill, 1968).
[9] J. J. Hopfield, Phys. Rev. B **112**, 1555 (1958).
[10] R. J. Donnelly and C. F. Barenghi, J. Phys. Chem. Ref. Data **27**, 1217 (1998).
[11] M. R. Moldover and W. A. Little, in *Critical phenomena*, edited by M. S. Green and J. V. Sengers (National Bureau of Standards Miscellaneous Publication, 1966) pp. 79–82.
[12] R. P. Feynman, Phys. Rev. **94**, 262 (1954).
[13] R. P. Feynman and M. Cohen, Phys. Rev. **102**, 1189 (1956).
[14] H. R. Glyde, Rep. Prog. Phys. **81**, 014501 (2018).
[15] H. Godfrin *et al.*, Phys. Rev. B **103**, 104516 (2021).
[16] R. A. Cowley and A. D. B. Woods, Can. J. Phys. **49**, 177 (1971).
[17] K. Beauvois *et al.*, Phys. Rev. B **94**, 024504 (2016).
[18] K. Beauvois *et al.*, Phys. Rev. B **97**, 184520 (2018).
[19] W. F. Vinen, Proc. Roy. Soc. A **260**, 218 (1961).
[20] W. F. Vinen, in *Superconductivity*, Vol. 2, edited by R. D. Parks (Dekker, New York, 1969) Chap. 20, pp. 1167–1234.
[21] S. C. Whitmore and J. W. Zimmermann, Phys. Rev. Lett. **15**, 389 (1965).